END
DATE
FILMED

10 83

DTIC

MICROCOPY RESOLUTION TEST CHART

NATIONAL BUREAU OF STANDARDS 1963 A

REPORT NO. NADC-81190-60

THE EFFECT OF SUPERPOSING RIPPLE LOADING
ON MANEUVER LOAD CYCLES

M. S. ROSENFELD
P. KOZEL
AIRCRAFT AND CREW SYSTEMS TECHNOLOGY DIRECTORATE
NAVAL AIR DEVELOPMENT CENTER
WARMINSTER, PA 18974

July, 1983

FINAL REPORT

AIRTASK WF41 400 000

DTIC
SELECTED
SEP 2 0 1983
A

AD-A132 653

DTIC FILE COPY

83 09 13 032
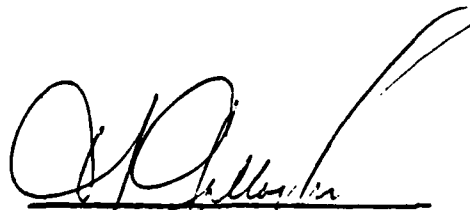
NADC-81190-60

N O T I C E S

REPORT NUMBERING SYSTEM - The numbering of technical project reports issued by the Naval Air Development Center is arranged for specific identification purposes. Each number consists of the Center acronym, the calendar year in which the number was assigned, the sequence number of the report within the specific calendar year, and the official 2-digit correspondence code of the Command Office or the Functional Directorate responsible for the report. For example: Report No. NADC-78015-20 indicates the fifteenth Center report for the year 1978, and prepared by the Systems Directorate. The numerical codes are as follows:
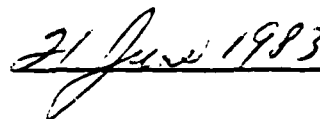
CODE	OFFICE OR DIRECTORATE
00	Commander, Naval Air Development Center
01	Technical Director, Naval Air Development Center
02	Comptroller
10	Directorate Command Projects
20	Systems Directorate
30	Sensors & Avionics Technology Directorate
40	Communication & Navigation Technology Directorate
50	Software Computer Directorate
60	Aircraft & Crew Systems Technology Directorate
70	Planning Assessment Resources
80	Engineering Support Group

PRODUCT ENDORSEMENT - The discussion or instructions concerning commercial products herein do not constitute an endorsement by the Government nor do they convey or imply the license or right to use such products.

APPROVED BY: _____   DATE: _21 June 1983_____

T. J. GALLAGHER
CAPTAIN, USN

REPORT DOCUMENTATION PAGE		READ INSTRUCTIONS BEFORE COMPLETING FORM
1. REPORT NUMBER NADC-81190-60	2. GOVT ACCESSION NO. AD-A132 653	3. RECIPIENT'S CATALOG NUMBER
4. TITLE (and Subtitle) The Effect of Superposing Ripple Loading on Maneuver Load Cycles		5. TYPE OF REPORT & PERIOD COVERED Final
		6. PERFORMING ORG. REPORT NUMBER
7. AUTHOR(s) M. S. Rosenfeld		8. CONTRACT OR GRANT NUMBER(s)
9. PERFORMING ORGANIZATION NAME AND ADDRESS Naval Air Development Center Warminster, PA 18974		10. PROGRAM ELEMENT, PROJECT, TASK AREA & WORK UNIT NUMBERS 62241N WF41-400, ZA61A
11. CONTROLLING OFFICE NAME AND ADDRESS Commander Naval Air Development Center Warminster, PA 18974		12. REPORT DATE February, 1983
		13. NUMBER OF PAGES 36
14. MONITORING AGENCY NAME & ADDRESS(If different from Controlling Office)		15. SECURITY CLASS. (of this report) UNCLASSIFIED
		15a. DECLASSIFICATION/DOWNGRADING SCHEDULE

16. DISTRIBUTION STATEMENT (of this Report)

Approved for public release; distribution unlimited

17. DISTRIBUTION STATEMENT (of the abstract entered in Block 20, If different from Report)

18. SUPPLEMENTARY NOTES

19. KEY WORDS (Continue on reverse side if necessary and identify by block number)

Fatigue	Spectrum Fatigue
Life Prediction	Load Superposition
Aircraft Structures	Cumulative Damage

20. ABSTRACT (Continue on reverse side if necessary and identify by block number)

This program was a systematic experimental investigation of the effect of superposing ripple loads on large amplitude cycles typical of aircraft maneuver loads. Since an adequate data base to define the magnitude and frequency of occurrence of ripple loads in service was not available, a range of values intended to represent a severe case was selected.

DD FORM 1473 1 JAN 73   EDITION OF 1 NOV 68 IS OBSOLETE
S/N 0102-LF-014-6601

From the results of this investigation it was concluded that:

1. Ripple load superposition reduces the constant-amplitude fatigue life of 7075-T6 aluminum but consistent, large life reductions were not apparent until ripple load amplitude exceeded 15% of the amplitude of the primary load cycles.

2. Similarly, superposition of ripple loading on the five highest load levels in a typical fighter/attack fatigue spectrum also reduces fatigue life, but the life reduction is more difficult to characterize in general terms.

3. Current methods of fatigue analysis which employ a local strain approach were able to predict the trends in fatigue life reduction caused by ripple loads with reasonable accuracy considering the scatter in the test data. However, they still had a tendency to underpredict the magnitude of the ripple effect.

TABLE OF CONTENTS

SYMBOLS

K_{tg}, stress concentration factor based on gross section stress

K_{tn}, stress concentration factor based on net section stress

t, specimen thickness, in.

w, specimen width, in.

A_{gr}, gross area

A_{net}, net area

S_{net}, net section stress

S_{gr}, gross section stress

P_{ult}, ultimate static strength, lbs.

S_{max}, maximum cyclic net section stress

S_{min}, minimum cyclic net section stress

S_R, net section stress due to ripple loading

B, superposed cycle ratio, cycles per cycle

N, number of cycles to failure

S_{1g}, net section stress at $n_z = 1g$

S_{LL}, net section stress at design limit load $n_z = 7.33g$

n_z, normal acceleration

L.L., limit load

LIST OF FIGURES

LIST OF TABLES

NADC-81190-60

FOREWORD

This program was performed in the Structures Research and Development
Branch, Aero Structures Division, Aircraft and Crew Systems Technology
Directorate, of the Naval Air Development Center. Mr. M. S. Rosenfeld
was the project engineer. Mr. Rosenfeld and Mr. P. Kozel coauthored
the report. The contributions of Mr. R. Vining of NAVAIRDEVCEN, Mr.
C. Saff and N. Austin of McDonnell Douglas Corporation for the fatigue
analysis, and Mr. H. Slavin for assisting with the test program are
gratefully acknowledged.

v

SUMMARY

This program was a systematic experimental investigation of the effect of superposing ripple loads on large amplitude cycles typical of aircraft maneuver loads. Since an adequate data base to define the magnitude and frequency of occurrence of ripple loads in service was not available, a range of values intended to represent a severe case was selected.

From the results of this investigation, it was concluded that:

1. Ripple load superposition reduces the constant-amplitude fatigue life of 7075-T6 aluminum but consistent, large life reductions were not apparent until ripple load amplitude exceeded 15% of the amplitude of the primary load cycles.

2. Similarly, superposition of ripple loading on the five highest load levels in a typical fighter/attack fatigue spectrum also reduces fatigue life, but the life reduction is more difficult to characterize in general terms.

3. Current methods of fatigue analysis which employ a local strain approach were able to predict the trends in fatigue life reduction caused by ripple loads with reasonable accuracy considering the scatter in the test data. However, they still had a tendency to underpredict the magnitude of the ripple effect, particularly for ripples of low amplitude.

INTRODUCTION

In-service load surveys of fighter/attack type aircraft show that typical high amplitude maneuver loads are often modulated by smaller amplitude loads which have a high frequency of occurrence (See Figure 1). These small amplitude, "ripple" loads are not included in aircraft fatigue test spectra and are not recorded by the current Navy fatigue life tracking system. The effect, on fatigue life, of these superimposed ripple loads in terms of their amplitude and frequency of occurrence is not well understood and could be a significant factor in developing realistic fatigue test spectra and more accurate fatigue life tracking systems.

This program was a systematic experimental investigation of the effect of ripple loads on fatigue life. A limited investigation of the ability of current fatigue life analyses to predict these effects was also performed.

TEST SPECIMENS

The test specimens used for this investigation are shown in Figure 2. The specimens were made from 0.125 in. thick 7075-T6 aluminum alloy sheet. Approximately 2.5 in. at each end of the specimen were used for gripping in the test machine.

2
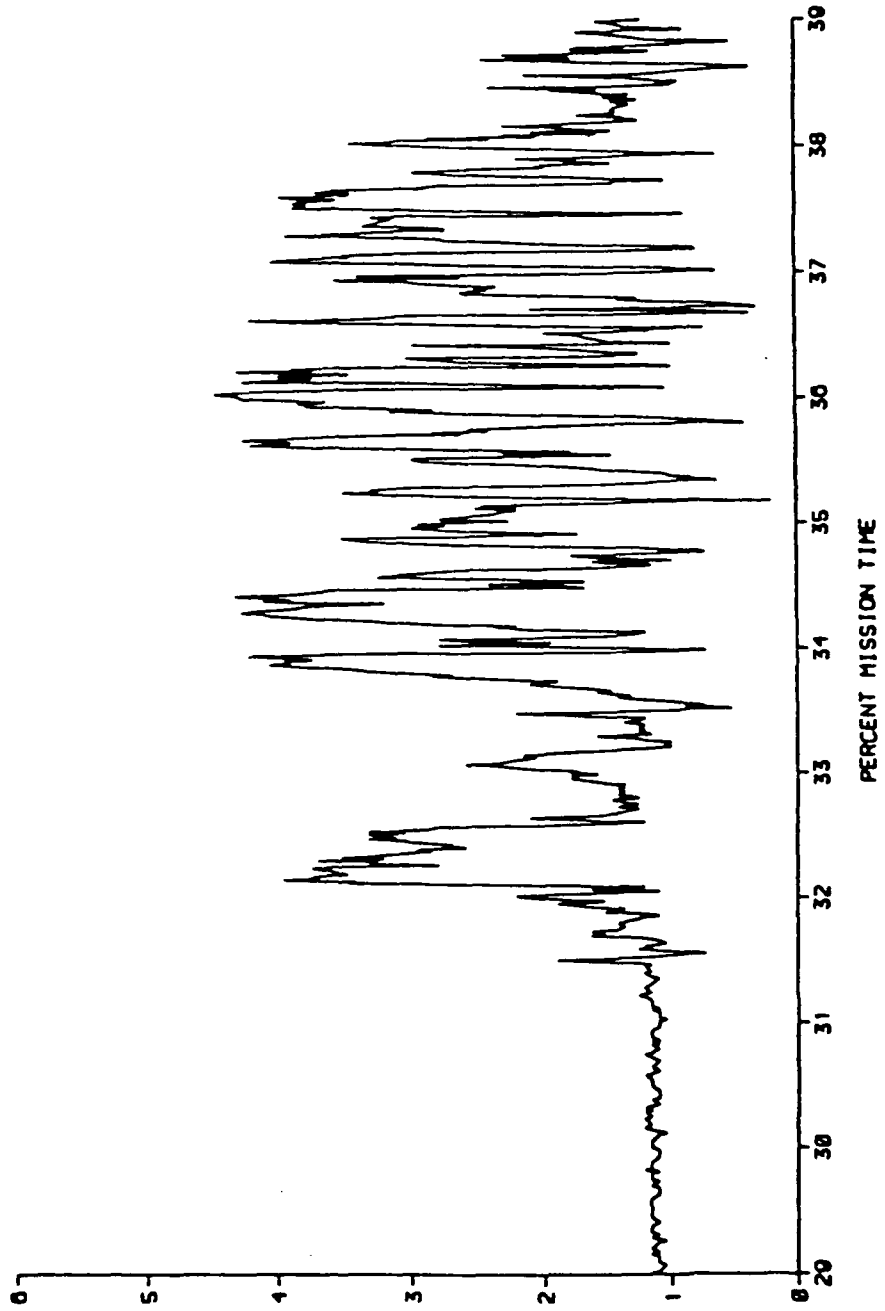
Figure 1 -- Ripple loads on a typical fighter/attack mission segment
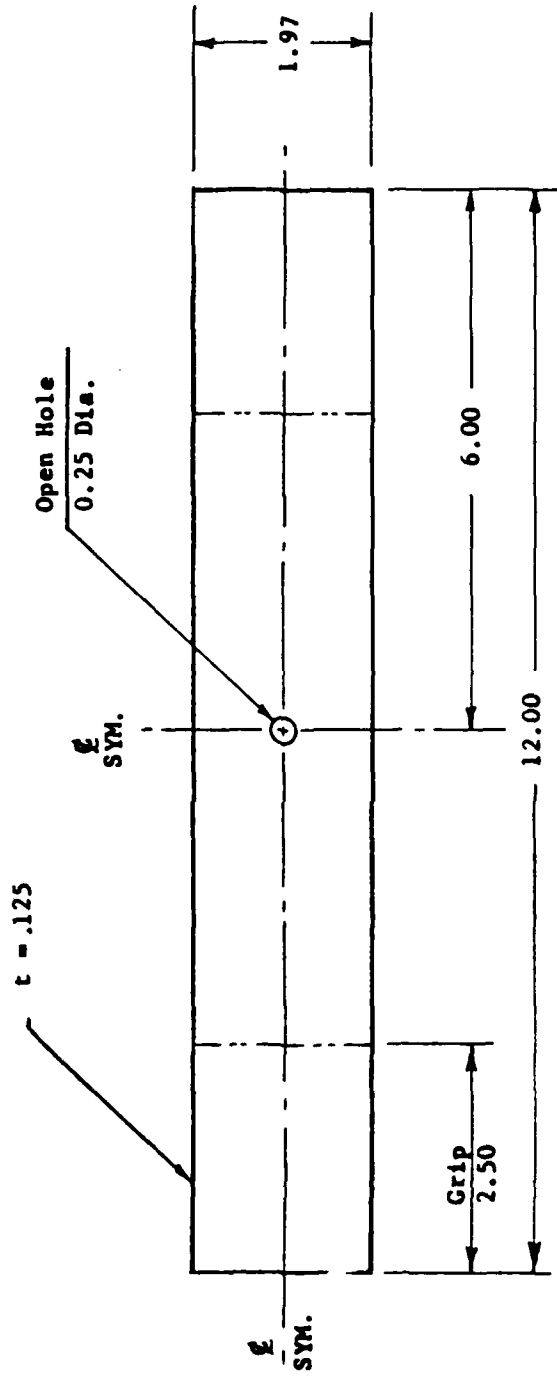
Figure 2 -- Test specimen

The nominal gross area of the specimen is 0.246 in.^{2} and the nominal net section area is 0.215 in.^{2} From Figure 86, Page 150 of Peterson[2], the stress concentration factor, K_{t_n}, based on net section stress is 2.67.

The static tensile strengths of the test specimens are given in Table 1.

TEST PROGRAM

The constant-amplitude test matrix is outlined in Table 2. The baseline test data were obtained for the trapezoidal loading cycles depicted in Figure 3. The 0.25 second interval between trapezoidal cycles was due to the program time limitations of the programmer. Although the trapezoidal loading cycle is not entirely representative of actual flight loading conditions, it was selected to simplify the analysis for the superposed loading condition. Additional baseline tests for the sinusoidal loading cycle shown in Figure 3(b) were performed to determine if the shape of the load cycle would influence the test results. As shown in Figure 4, the constant-amplitude lives for the sinusoidal and trapezoidal cycle shapes are essentially identical. The shape of the load waveform with ripple loads superposed upon the trapezoidal loading is shown in Figures 3(c), (d), and (e).

The spectrum loading test matrix is shown in Table 3. The spectrum used corresponds to the fighter spectrum A of MIL-A-8866 (ASG) with an assumed limit load factor n_z = 7.33g. Because of the capacity limitation of the load programmer, the spectrum was limited to positive loads only

NADC-81190-60

TABLE 1

SPECIMEN STATIC STRENGTH

SPEC. NO.	t (in.)	w (in.)	A_{gr} (in.^{2})	A_{net} (in.^{2})	P_{ult} (lbs.)	S_{net} (ksi)	S_{gr} (ksi)
S-2	.1258	1.9705	.24789	.21644	18100	83.63	73.02
S-3	.1256	1.9714	.24761	.21621	17940	82.97	72.45
S-4	.1255	1.9736	.24769	.21631	18060	83.49	72.91
AVERAGE						83.36	72.79

6

TABLE 2

CONSTANT AMPLITUDE TEST MATRIX

	CYCLE SHAPE	FIG. 3 REF.	RIPPLE STRESS S_R (ksi)	MAXIMUM CYCLIC STRESS, S_{max} (KSI)									
				48	44	40	36	32	28	24	22	20	16
BASELINE	TRAPEZOIDAL	(a)	0	3(1)	3	3	3	3	3	3	4	2	-
	SINUSOIDAL	(b)	0		2	3		2		2			
SUPERPOSED	B = 1	(c)	4		3		3		3		3	3	
			8		3		3		3		3	3	
			12		3		3		3		3	3	
	B = 2	(d)	4		3		3		3		3	3	
			8		3		3		3		3	3	
			12		3		3		3				
	B = 4	(e)	4		3		3		3		3	4	3
			8		3		3		3		3	3	
			12				3		3		3	3	

(1) Number of replicate specimens for each loading condition and stress level.

7

(b.) Sinusoidal

(a.) Trapezoidal

(c.) Superposed, B = 1

(d.) Superposed, B = 2
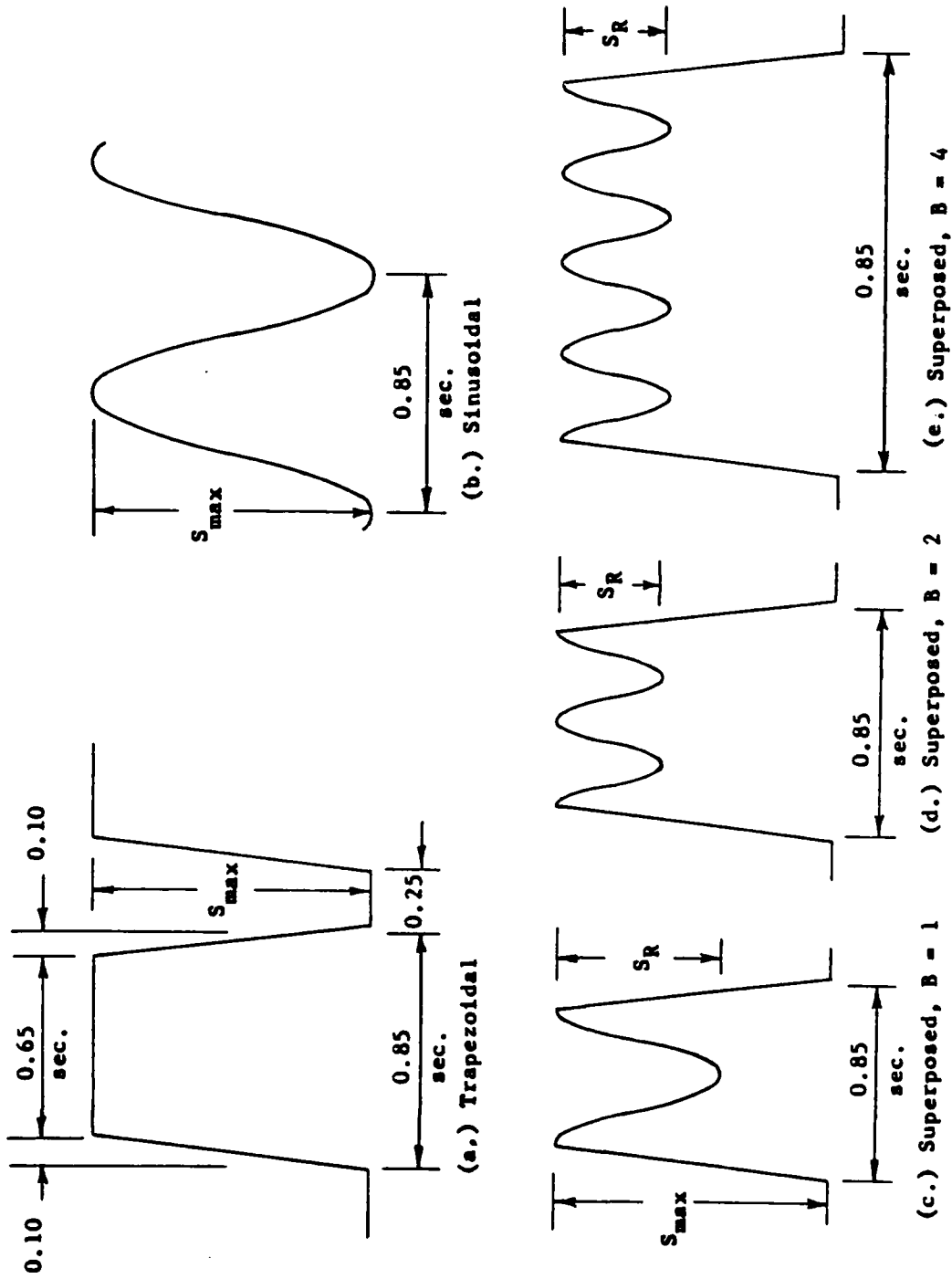
(e.) Superposed, B = 4

Figure 3 -- Loading cycle shapes

and was applied in 50 hr. equivalent blocks as follows:

% L.L.	35	45	55	65	75	85	95	105	115	125
N	850	475	325	225	125	75	15	8	2	1
f(Hz)	5	5	5	4	4					

Because of the capacity limitation of the load programmer, the super-posed sinusoidal ripple loading was applied to the 85% and higher load levels only. The lower load level for each cycle was zero rather than the load corresponding to the level flight 1g load to simplify the load cycle and to make it compatible with the constant-amplitude cycling.

The baseline test data were obtained for the spectrum shown above with the cycles between 35% and 75% limit load applied sinusoidally at the frequencies noted. Cycles at 85% limit load and above were trapezoidal so that sinusoidal ripple loading could be superposed as for the constant-amplitude tests. The tests were performed for four different stress levels, S_{1g}, as shown in Table 3; the corresponding limit load stresses, S_{LL}, are also shown.

TEST METHOD

All tests were performed in a 20 Kip closed-loop servohydraulic test machine equipped with self-aligning hydraulic grips. The test loads were monitored throughout by an amplitude measuring unit utilizing both an oscilloscope and a peak reading digital voltmeter.

All test data is reported as life to failure and therefore includes both the crack initiation and crack growth stage.

TABLE 3

SPECTRUM LOADING TEST MATRIX

	RIPPLE STRESS S_R (KSI)		SPECTRUM STRESS LEVEL (KSI)			
		S_{1g}	4.0	4.4	4.8	5.2
		S_{LL}	29.32	32.25	35.18	38.12
BASELINE	0	B = 0	2	2	2	2
	4		2	2	2	2
	8	B = 1	2	2	2	2
	12		4	2	2	2
SUPERPOSED	4		2	2	2	2
	8	B = 2	2	2	2	2
	12		2	2	2	2
	4		2	2	2	2
	8	B = 4	2	2	2	4
	12		4	4	4	4

TEST RESULTS AND DISCUSSION

Constant Amplitude Loading

The baseline (B = 0), constant amplitude date for a trapezoidal and sinusoidal loading cycle are given in Table 4 and plotted in Figure 4. It is apparent, from the latter, that cycle shape has no effect.

Results for the constant amplitude ripple load test matrix are presented in Tables 5 thru 7 and plotted in Figures 5 through 9. While some trends can be perceived in this data (mean life curves are shown), the data scatter and small sample size make conclusions precarious, especially in interpreting the effect of the smallest, i.e., 4 ksi ripples. In order to unify the results, the mean life data for each ripple condition was normalized with respect to the mean ripple-free (B = 0), life at each level of maximum stress. The normalized results are given in Table 8. Again, it is apparent that some of the results are anomalies. For example, the life ratio for S_R = 4, B = 2 is higher than for S_R = 4, B= 1. However, ripple loads above 8 ksi in amplitude produce a substantial reduction in life with the greater reduction, as would be expected, evident at higher amplitudes and higher ripple ratios.

Spectrum Loading

Spectrum test results are given in Table 9 and are plotted in Figures 10 thru 13. These test results are normalized to the mean

TABLE 4

LIFE TO FAILURE
CONSTANT AMPLITUDE LOADING
BASELINE DATA, B = 0

S_{max} (KSI)	LIFE, N - CYCLES		S_{max} (KSI)	LIFE, N - CYCLES	
	TRAPEZOIDAL	SINUSOIDAL		TRAPEZOIDAL	SINUSOIDAL
48	4144 3625 3942 3904 av.		28	24885 24169 27627 25560 av.	
44	6303 5390 5300 5664	4573 6174 5376	24	37900 52006 36817 42241	50874 40805 45840
40	8650 7909 8451 8337	6126 9575 6863 7521	22	265248(1) 65091 57983 79728 67601	
36	12195 13092 11247 12178		20	>573843 >542346	
32	15667 16810 15090 15856	20538 14375 17456			

(1) Failed in grips - not included in average values.

12
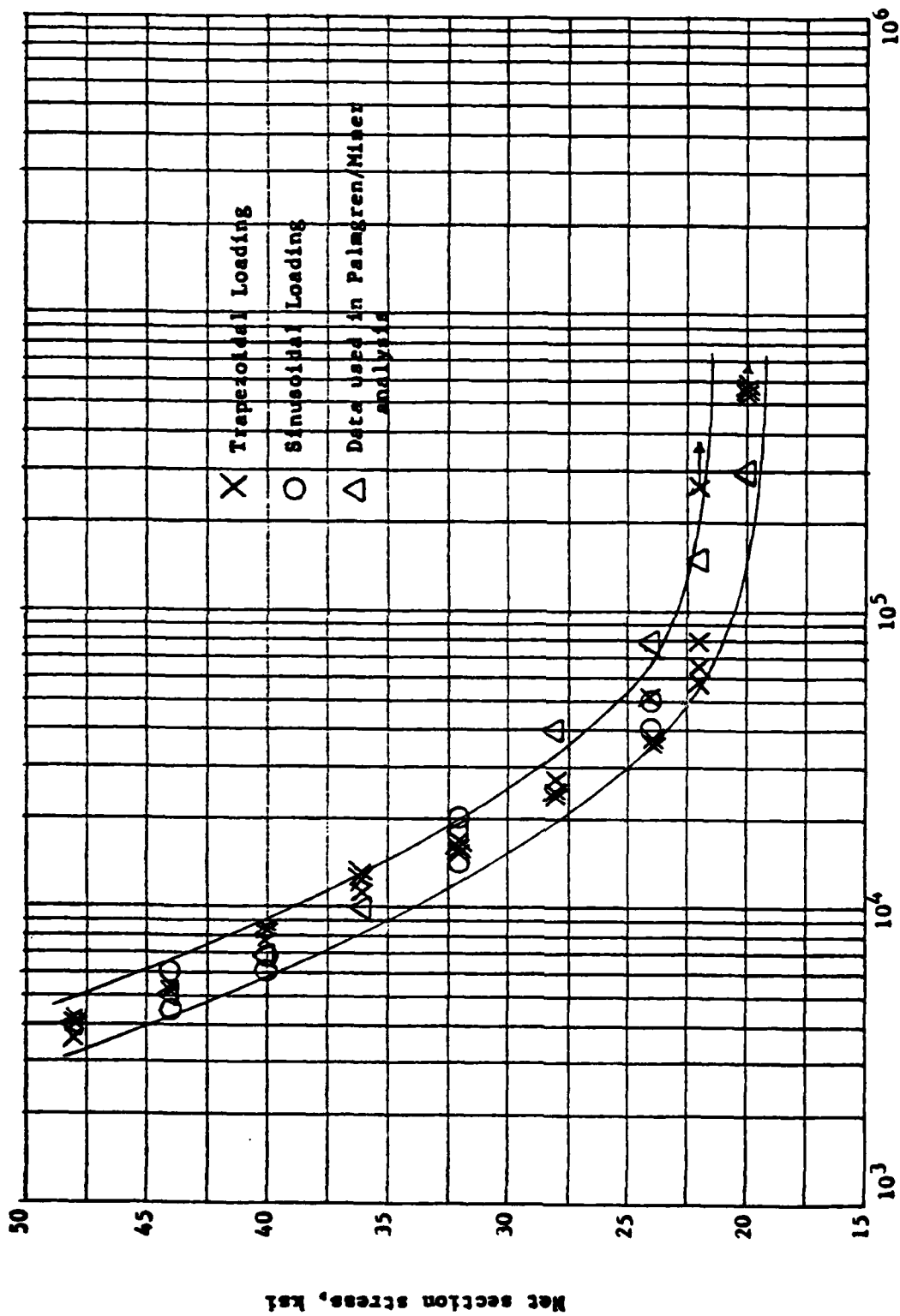
N, Cycles to failure

Figure 4 -- Life to failure, constant amplitude loading (baseline data)

TABLE 5

LIFE TO FAILURE
CONSTANT AMPLITUDE LOADING

SUPERPOSED CYCLE RATIO, B = 1

S_{max} (ksi)	LIFE TO FAILURE, N_T - CYCLES		
	S_R = 4 ksi	S_R = 8 ksi	S_R = 12 ksi
44	3922 3937 <u>3686</u> 3848 av.	3444 3671 <u>3656</u> 3590 av.	3190 3750 <u>3228</u> 3389 av.
36	8633 9021 <u>8321</u> 8658	8209 6915 <u>7067</u> 7397	6581 6338 <u>7458</u> 6792
28	18731 19126 <u>17678</u> 18512	16820 17128 <u>14578</u> 16175	13505 15211 <u>20034</u> 16250
22	53839 56368 <u>58525</u> 56244	35411 35828 <u>37485</u> 36241	39271 32786 <u>24670</u> 32242
20	135266 61808 <u>86219</u> 94431	51860 44082 <u>48520</u> 48154	84327 29872 <u>43202</u> 52467

TABLE 6

LIFE TO FAILURE
CONSTANT AMPLITUDE LOADING
SUPERPOSED CYCLE RATIO, B = 2

S_{max} (ksi)	LIFE TO FAILURE, N_T - CYCLES		
	S_R = 4 ksi	S_R = 8 ksi	S_R = 12 ksi
44	4146 5894 <u>6134</u> 5391 av.	4196 .3813 <u>4256</u> 4088 av.	4167 4287 <u>3658</u> 4037 av.
36	10611 12863 <u>9927</u> 11134	8407 9533 <u>7842</u> 8594	6829 7843 <u>6282</u> 6985
28	35788 22798 <u>22656</u> 27081	23295 .28928 <u>27651</u> 26625	16282 8476 <u>11268</u> 12009
22	44582 62759 <u>90394</u> 65912	29582 31246 <u>24521</u> 28450	
20		34941 56654 <u>51853</u> 47816	34256 32629 <u>26491</u> 31125
16			61665 46222 <u>53363</u> 53747

TABLE 7

LIFE TO FAILURE
CONSTANT AMPLITUDE LOADING

SUPERPOSED CYCLE RATIO, B = 4

S_{max} (ksi)	LIFE TO FAILURE, N_T - CYCLES		
	$S_R = 4$ ksi	$S_R = 8$ ksi	$S_R = 12$ ksi
44	3881 4190 <u>4439</u> 4170 av.	3419 3434 <u>3186</u> 3346 av.	2873 3331 <u>3083</u> 3096 av
36	6448 10647 <u>9015</u> 8703	6828 7887 <u>6513</u> 7076	5504 4785 <u>5275</u> 5188
28	18903 23562 <u>16522</u> 19662	11606 13938 <u>13492</u> 13012	8408 10698 <u>9559</u> 9555
22	36663 45944 <u>64350</u>[1] 41304	23548 28385 <u>23175</u> 25036	21298 14912 <u>27456</u> 21222
20	269748[1] 526745[1] 48318 <u>57735</u> 53026	43619 67820[1] 75375[1] ___ 43619	16331 36214 17007 ___ 23184

(1) Specimen failed in grips; not used in determining average value.
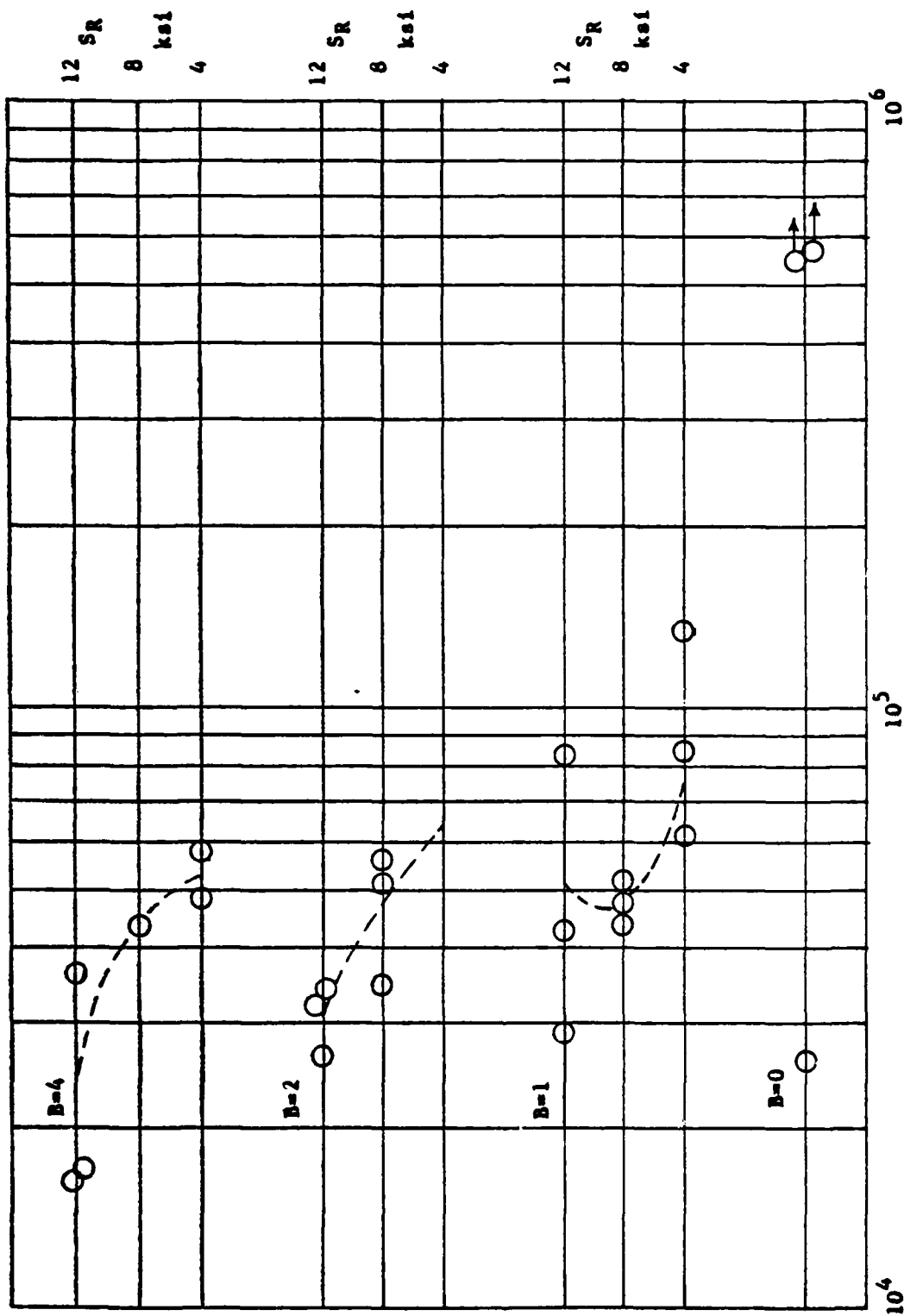
Figure 5 -- Constant amplitude loading, SMAX = 20 ksi.
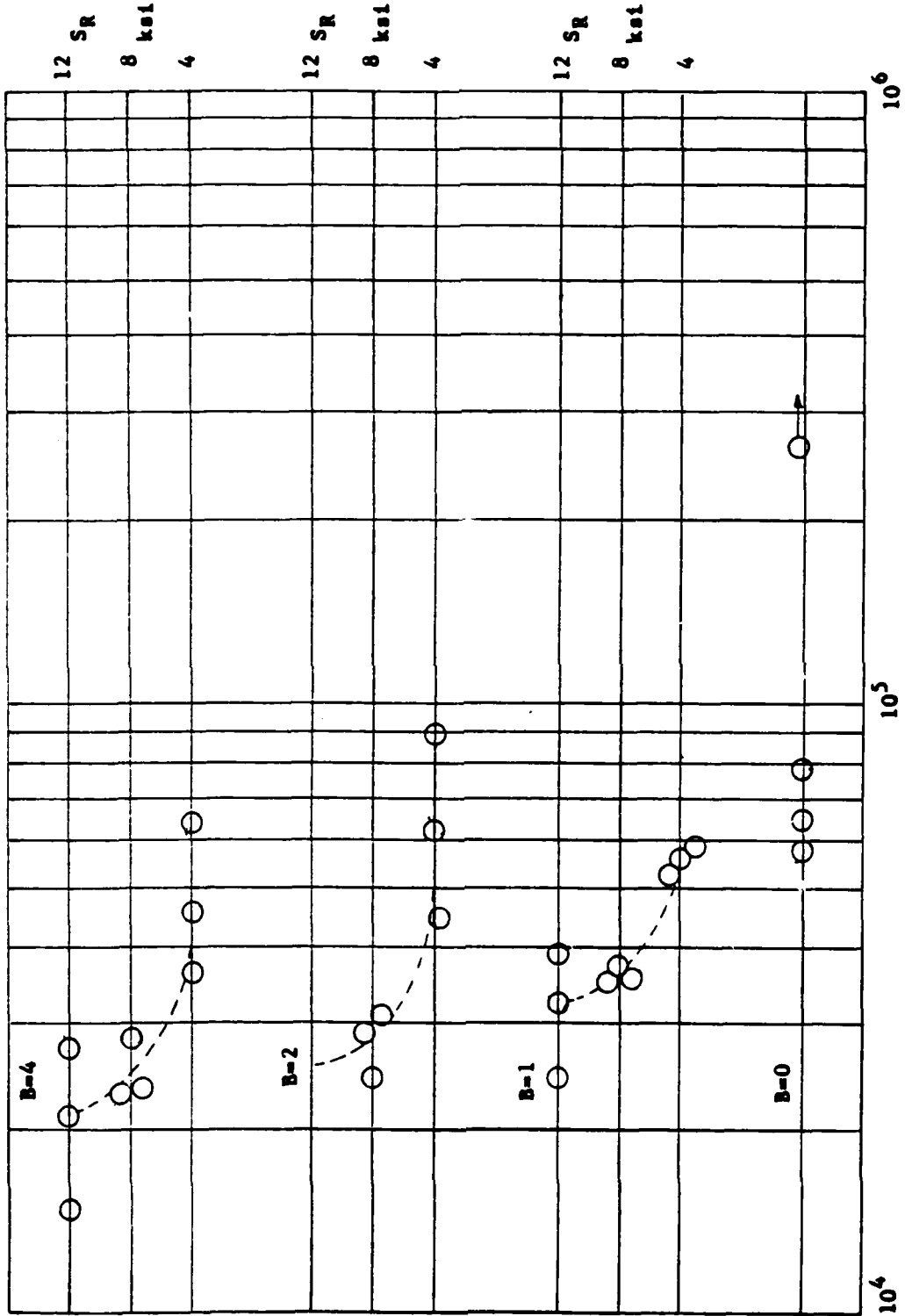
Figure 6 -- Constant amplitude loading, SMAX = 22 ksi.
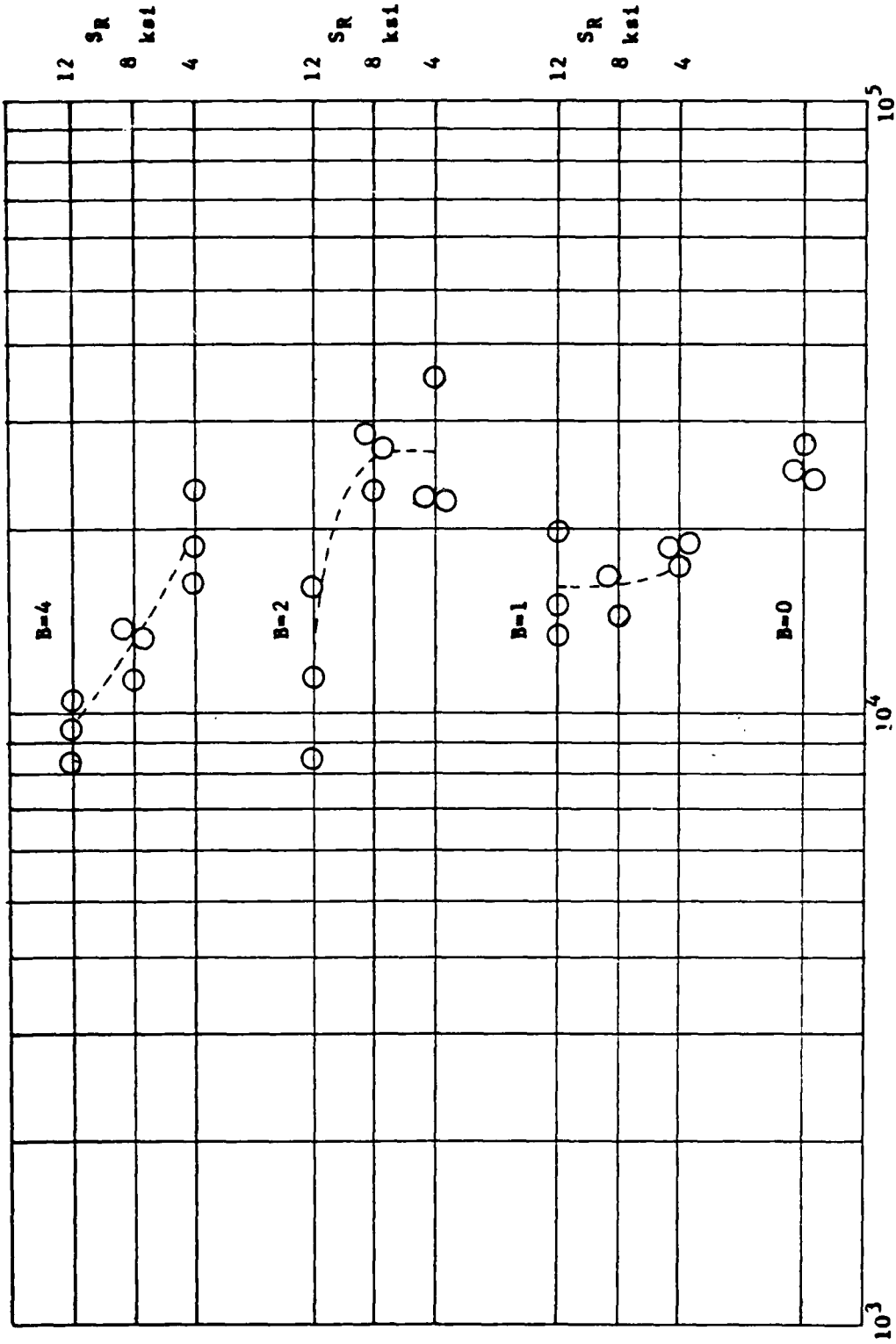
Figure 7 -- Constant amplitude loading, SMAX = 28 ksi.
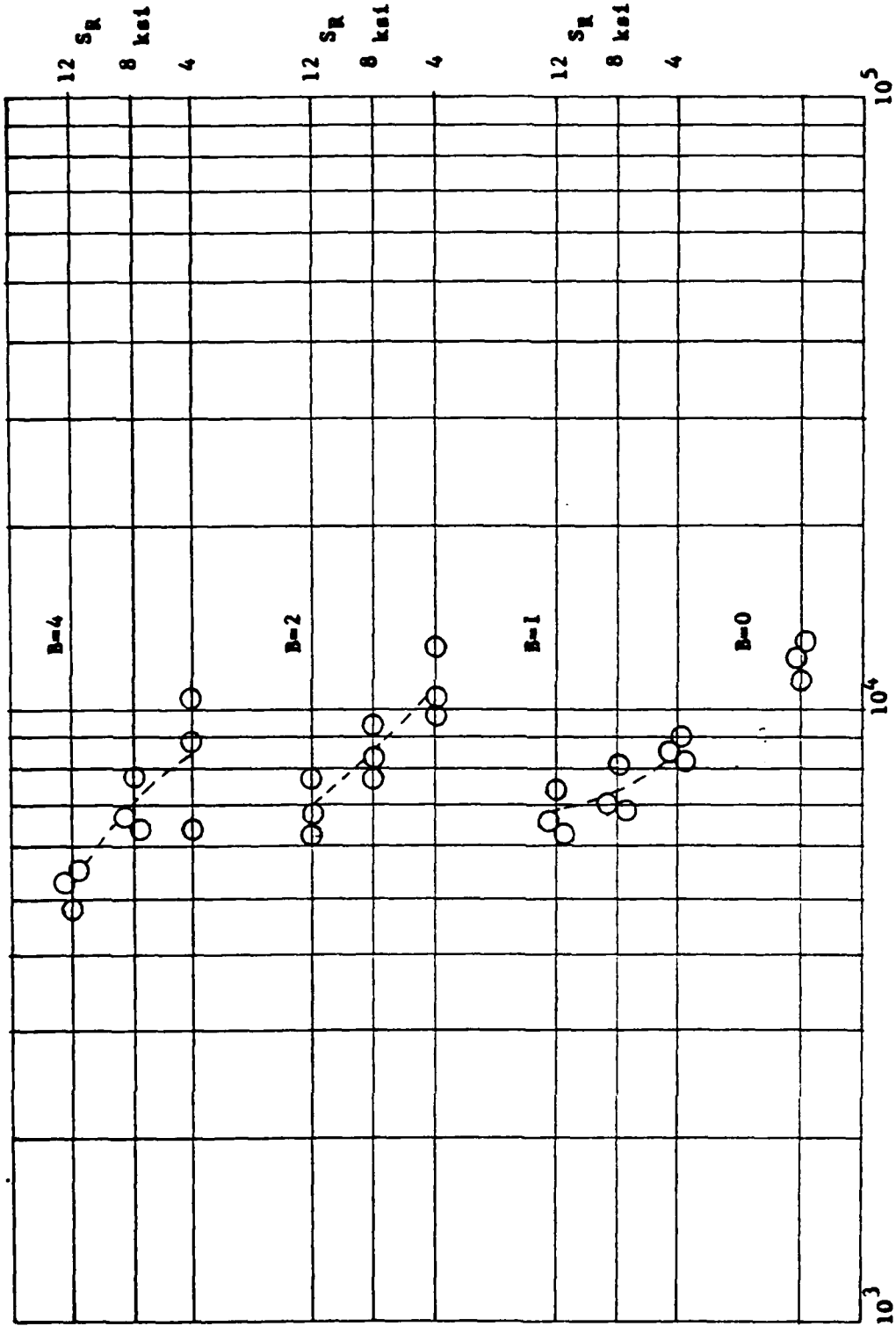
Figure 8 -- Constant amplitude loading, SMAX = 36 ksi.
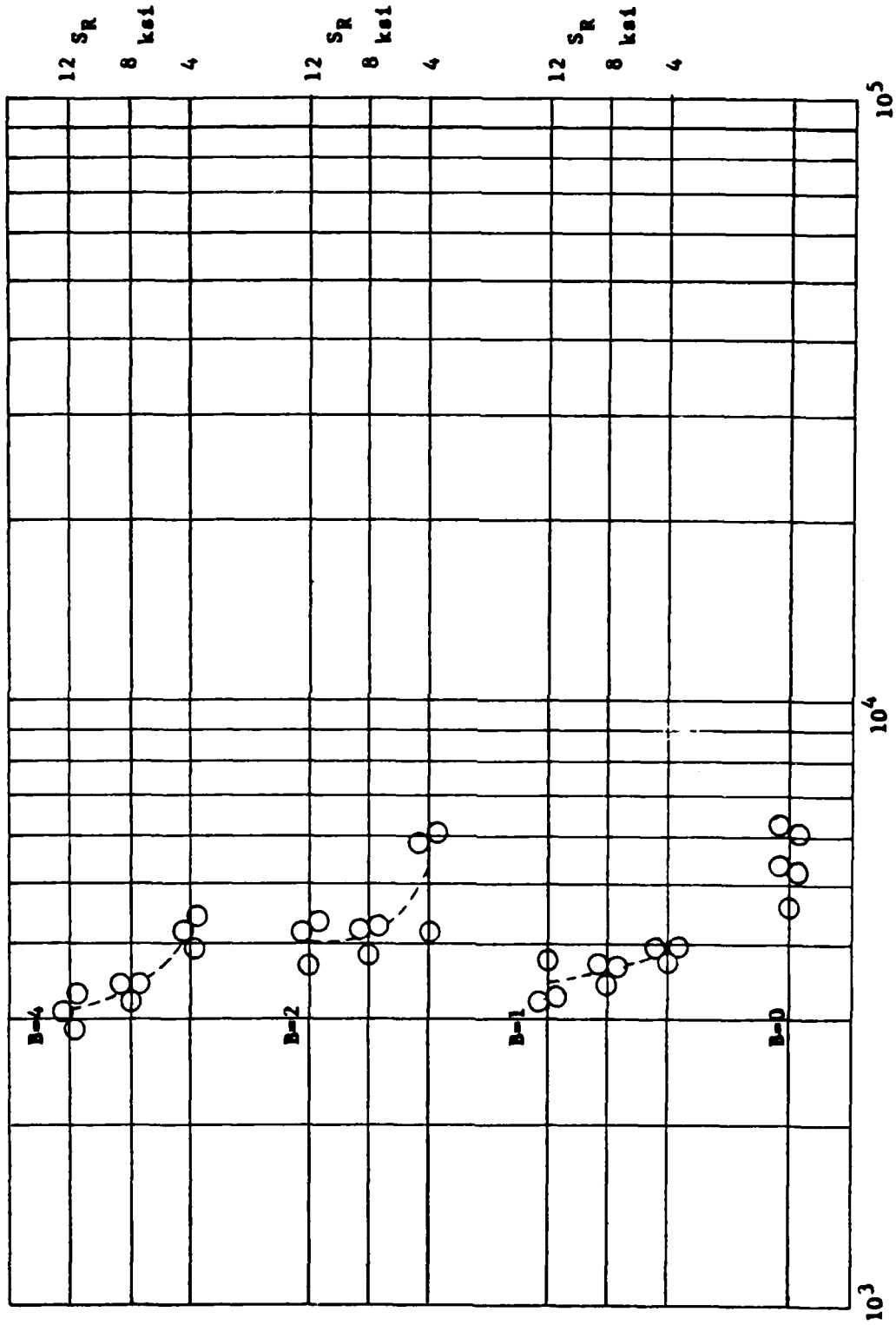
N, Cycles to failure

Figure 9 -- Constant amplitude loading, SMAX = 44 ksi.

21

TABLE 8

LIFE RATIOS

CONSTANT AMPLITUDE LOADING WITH RIPPLES

B	S_R (ksi)	S_{max} (ksi)			
		44	36	28	22
Baseline	0	1.000	1.000	1.000	1.000
1	4	0.679	0.711	0.724	0.832
	8	0.634	0.607	0.633	0.536
	12	0.598	0.558	0.636	0.477
2	4	0.952	0.914	1.060	0.975
	8	0.722	0.706	1.042	0.421
	12	0.713	0.574	0.470	-
4	4	0.736	0.715	0.769	0.611
	8	0.591	0.581	0.509	0.370
	12	0.547	0.426	0.374	0.314

TABLE 9

SPECTRUM LOADING TEST RESULTS

B	S_R (ksi)	LIFE TO FAILURE, N_B - 50 HR. BLOCKS			
		S_{1g} =4.0 ksi	S_{1g} =4.4 ksi	S_{1g} =4.8 ksi	S_{1g} =5.2 ksi
Baseline	0	472 360 416 av.	296 247 271.5 av.	313 197 255 av.	180 138 159 av.
1	4	523 481 502	277 251 264	196 219 207.5	171 168 169.5
	8	382 446 414	324 297 310.5	193 219 206	163 171 167
	12	210 129 152 142 158.2	304 179 241.5	111 144 127.5	140 115 127.5
2	4	372 376 374	310 338 324	199 221 210	171 171 171
	8	411 429 420	270 255 262.5	182 193 187.5	161 172 166.5
	12	176 220 198	203 145 174	107 170 138.5	123 107 115
4	4	389 424 406.5	301 281 291	179 180 179.5	162 158 160
	8	374 316 345	248 189 218.5	140 156 148	166 164 110 98 134.5
	12	95 92 73 101 90.2	137 104 140 100 120.2	81 72 88 108 87.2	60 41 89 102 73

Figure 10 -- Spectrum loading, SIG = 4.0 ksi.
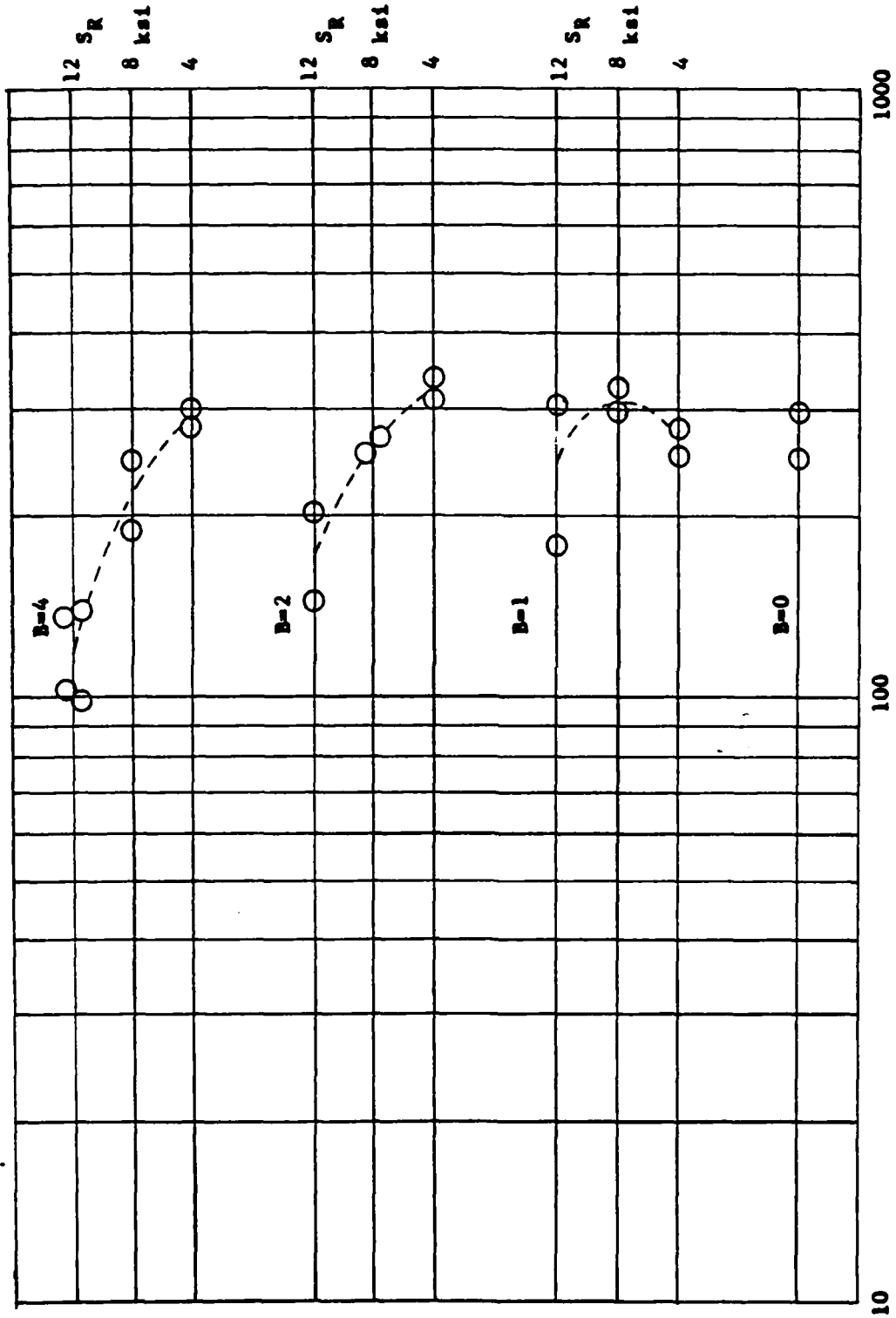
Blocks to failure

Figure 11 -- Spectrum loading, SIG = 4.4 ksi.

12 S_R

8 ksi

4

12 S_R

8 ksi

4

12 S_R

8 ksi

4

1000

B=4

B=2

B=1

B=0

100

Blocks to failure

Figure 12 -- Spectrum loading, SIG = 4.8 ksi

10

Figure 13 -- Spectrum loading, SIG = 5.2 ksi

ripple-free (B = 0) life at each spectrum stress level in Table 10.
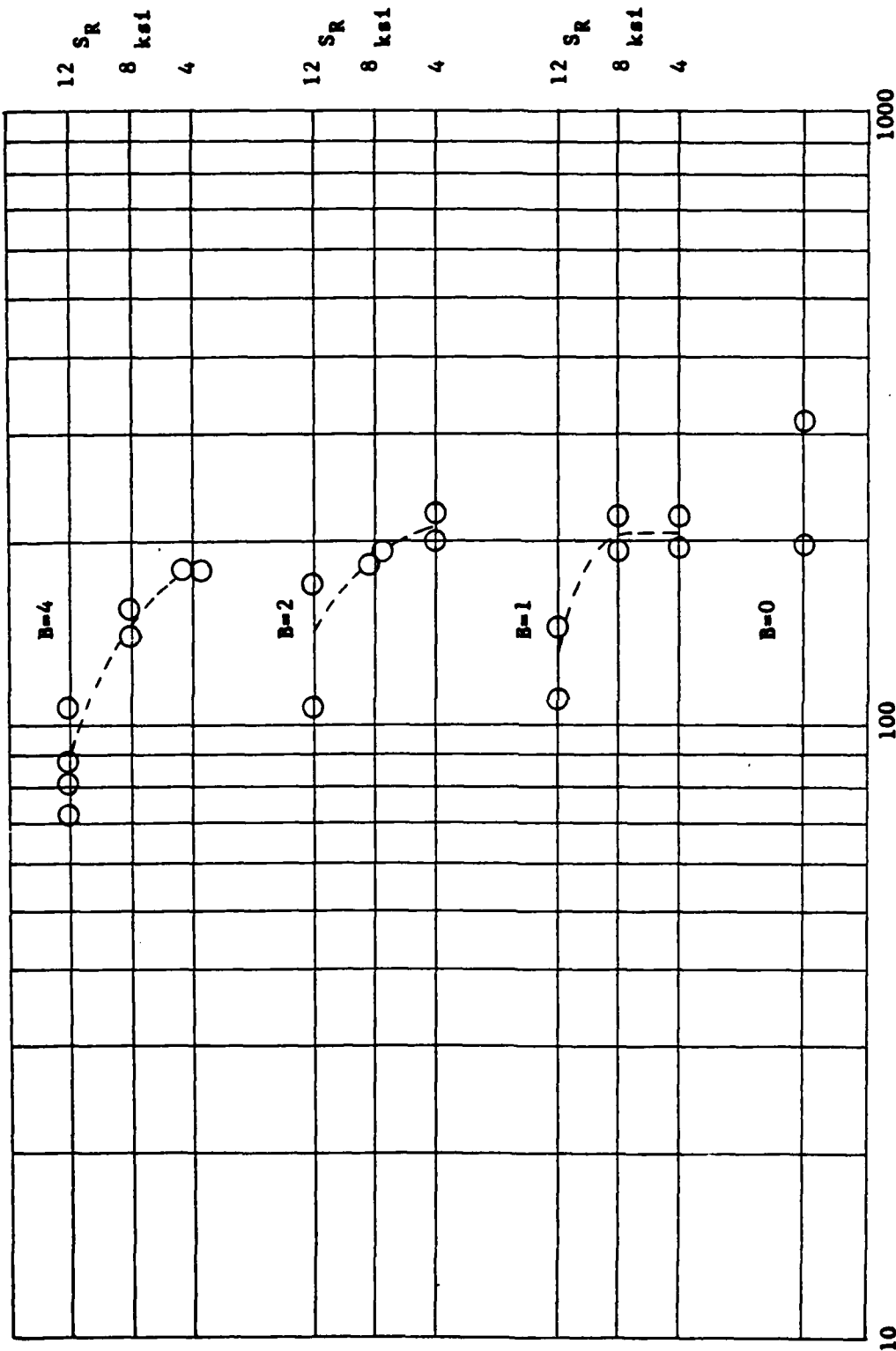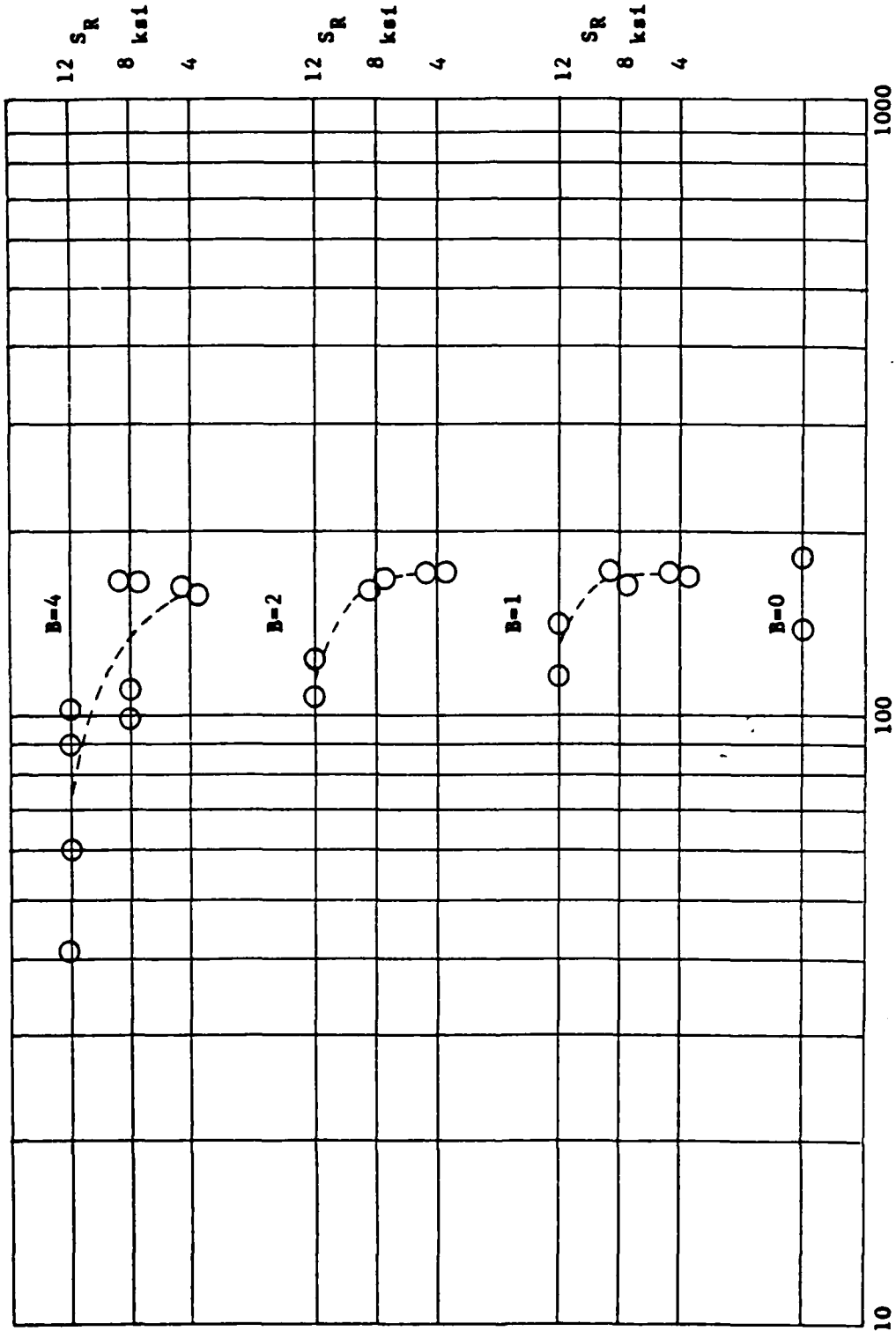These results also show negligible life reduction caused by ripple loads
until the ripple amplitude exceeds 8 ksi. Under these test conditions,
where spectrum design limit stress ranged from 29 ksi to 38 ksi, an
8 ksi ripple cycle is a relatively large percentage of limit stress
and a significant life reduction would be expected.

ANALYSIS RESULTS

Fatigue life tracking systems now being proposed for Navy aircraft
will measure and record stress ripples which exceed 15% of design limit
stress (see References 1 and 6). It therefore becomes an important
question whether the accompanying fatigue analysis can account for the
ripple effects.

Two types of analysis were applied to selected ripple test
conditions. The first was the Palmgren-Miner linear cumulative damage
approach, and the second was a typical sequence accountable method
which tracks the local stress/strain history by modelling the hysteresis
loops. The Palmgren-Miner analysis was applied using S vs. N data for
7075-T6 derived from MIL-HDBK-5C (See Figure 4). The sequence accountable
method used existing stress/strain vs. life data for 7075-T6.

Total life predictions in general were poor, tending to be highly
conservative unless the predictions were matched, ex-post-facto, to the
ripple-free test data. Miner's analysis, however, was non-conservative for

TABLE 10

LIFE RATIOS SPECTRUM LOADING

WITH RIPPLES

B	S_R (ksi)	S_{1g} = 4.0 ksi	S_{1g} = 4.4 ksi	S_{1g} = 4.8 ksi	S_{1g} = 5.2 ksi
Baseline	0	1.000	1.000	1.000	1.000
1	4	1.207	0.972	0.814	1.066
	8	0.995	1.144	0.808	1.050
	12	0.380	0.890	0.500	0.802
2	4	0.899	1.193	0.824	1.075
	8	1.010	0.967	0.735	1.047
	12	0.476	0.641	0.543	0.723
4	4	0.977	1.072	0.704	1.006
	8	0.829	0.805	0.580	0.846
	12	0.217	0.443	0.342	0.459

conditions of S_{max} = 28 ksi where large scatter is evident in the test data. To display the sensitivity of the analysis methods to the ripple effects, the predictions were normalized to the ripple-free life. Comparisons between the test life ratio and predicted life ratio for selected constant amplitude and spectrum conditions are presented in Tables 11 and 12. Figure 14 shows a graphical comparison of test life vs. predictions by a sequence accountable analysis. The comparisons show that a simple Miner's analysis, in general, underpredicted the ripple effect for both constant amplitude and spectrum loading. The sequence accountable method was more sensitive to the ripple effect and gave life ratios which were reasonable, considering the scatter and sometimes inconsistent trends in the test data.

TABLE 11

LIFE RATIOS, TEST/ANALYSIS COMPARISONS

CONSTANT AMPLITUDE LOADING

B	S_R	$S_{max} = 44$		$S_{max} = 36$		$S_{max} = 28$		$S_{max} = 22$		
		TEST	P/M	TEST	P/M	TEST	P/M	TEST	P/M	SAA
0	0	1.00	1.00	1.00	1.00	1.00	1.00	1.00	1.00	1.00
1	4	.68	1.00	.71	1.00	.72	1.00	.83	1.00	.98
1	8	.63	.94	.61	.99	.63	1.00	.54	1.00	.92
1	12	.60	.89	.56	.90	.64	.96	.48	1.00	.81
2	4	.95	1.00	.91	1.00	1.06	1.00	.98	1.00	.97
2	8	.72	.89	.71	.98	1.04	1.00	.42	1.00	.85
2	12	.71	.80	.57	.82	.47	.93	-	.99	.68
4	4	.74	1.00	.72	1.00	.77	1.00	.61	1.00	.94
4	8	.59	.80	.58	.96	.51	1.00	.37	1.00	.74
4	12	.55	.67	.43	.69	.37	.89	.31	.98	.52

P/M = Palmgren/Miner Analysis

SAA = Sequence Accountable Analysis

TABLE 12

LIFE RATIOS, TEST/ANALYSIS COMPARISONS

SPECTRUM LOADING

B	S_R	$S_{lg} = 4.0$			$S_{lg} = 4.4$			$S_{lg} = 4.8$			$S_{lg} = 5.2$	
		TEST	P/M	SAA	TEST	P/M	SAA	TEST	P/M	SAA	TEST	P/M
0	0	1.00	1.00	1.00	1.00	1.00	1.00	1.00	1.00	1.00	1.00	1.00
1	4	1.21	1.00	-	.97	1.00	-	.81	1.00	-	1.06	1.00
	8	1.00	1.00	.92	1.14	1.00	-	.81	.99	-	1.05	.98
	12	.38	.97	.83	.89	.96	-	.50	.94	-	.80	.93
2	4	.90	1.00	.94	1.19	1.00	-	.82	1.00	-	1.08	1.00
	8	1.01	1.00	.85	.97	.99	-	.74	.99	-	1.05	.98
	12	.48	.94	.71	.64	.92	-	.54	.90	-	.72	.90
4	4	.98	1.00	.88	1.07	1.00	-	.70	1.00	-	1.01	1.00
	8	.83	1.00	.73	.80	.99	-	.58	.97	-	.85	.95
	12	.22	.89	.52	.44	.86	.42	.34	.82	.46	.46	.79

P/M = Palmgren/Miner Analysis
SAA = Sequence Accountable Analysis

Life
Ratio

Test Points

○ B=1

△ B=2

□ B=4

B = 1

B = 2

B = 4

Ripple Stress, S_R ksi

(a) Constant amplitude loading, SMAX=22ksi

Life
Ratio

Test Points

○ B=1

△ B=2

□ B=4

B = 1

B = 2

B = 4

Ripple Stress, S_R ksi
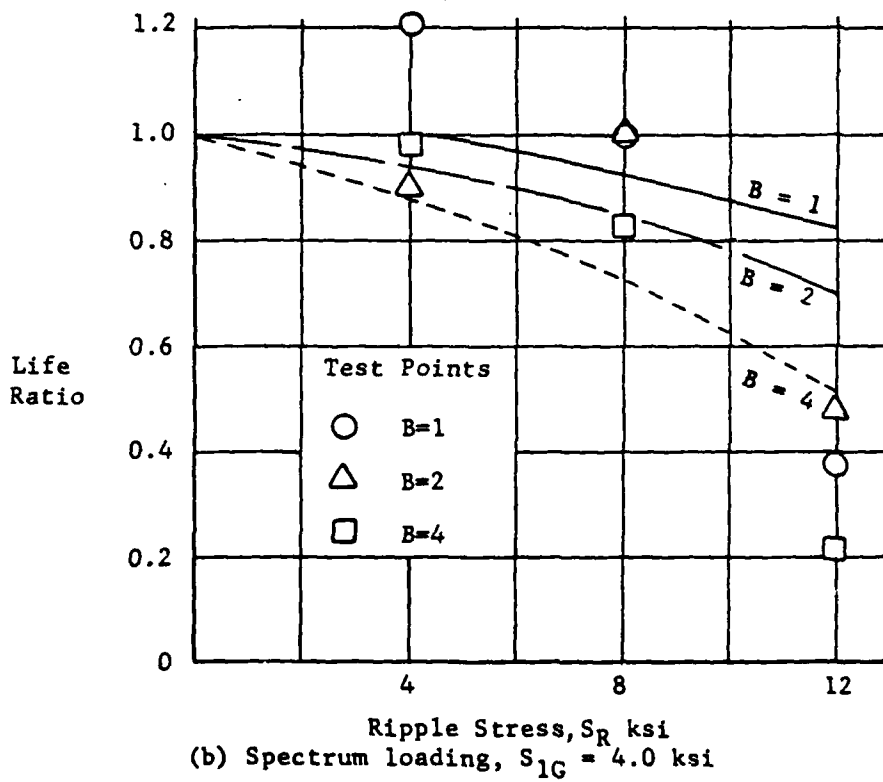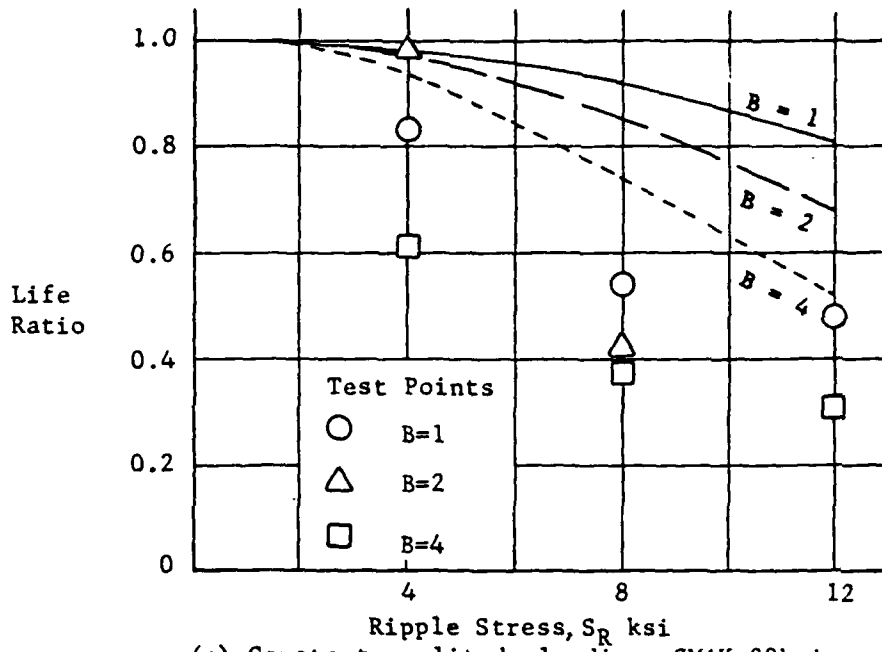
(b) Spectrum loading, S_{1G} = 4.0 ksi

Figure 14 - Life Ratios; Comparison of Test Life vs.
Sequence Accountable Analysis

CONCLUSIONS

An experimental investigation was performed to determine the effect on fatigue life of superposing small amplitude ripple load cycles on the larger amplitude cycles characteristic of aircraft maneuver loads. Two fatigue life prediction methods were also investigated to determine whether they could predict ripple load effects. From the results of this program, it is concluded that:

1. While ripple load superposition reduces the constant amplitude fatigue life of 7075-T6 aluminum, consistent large life reductions were not apparent until the ripple load amplitude exceeded 15% of the amplitude of the primary cycles and the number of ripples exceeded 2 cycles per cycle.

2. Superposition of ripple loads on the five highest load levels of the MIL-A-8866 (ASC) fighter/attack spectrum also reduces fatigue life, but the life reduction is more difficult to characterize in general terms because of the complexity of the spectrum and the scatter in the test data.

3. Miner's analysis, in general, underpredicted the life reductions produced by ripple loads for both constant amplitude and spectrum tests. A sequence accountable fatigue life prediction which tracks the local notch stress/strain history was more sensitive to the ripple effect and gave reasonable predictions of the ripple-free to ripple-imposed life ratios considering the small sample size and scatter of the test data. However, the sequence accountable analyses also tended to underpredict the magnitude of the life reductions produced by ripple loads.

34

RECOMMENDATIONS

Results of this experimental study show that ripple loads can have a significant effect on structural life; however, the amplitude and frequency-of-occurrence of ripple cycles in this study were relatively severe and may not be representative of the real service environment. It is recommended that airloads data from existing sources, such as operational surveys and the Tactical Aircrew Combat Training System, be reviewed to determine actual ripple load content and its effect on structural life.

Customary life prediction analyses tend to underpredict the actual effect of low amplitude ripples. This inaccuracy may be of greater consequence in predicting the life of transport/patrol type aircraft which experience numerous low-amplitude gust cycles. The introduction and decay of local residual stress is an aspect of fatigue analysis which affects the accuracy of structural life predictions for this type of load spectra, but the phenomenon is not well understood. Research into residual stress behavior, perhaps with instrumented super-scale specimens, would improve the accuracy of fatigue analysis for applications to gust loading and to other unusual spectra such as those containing ripple loads.

Other research (Reference 7), has shown that ripple-type loading can have a significant effect on the crack propagation stage of structural life. Since crack propagation analysis is now commonly used to protect aircraft safety during service life extensions, it should be determined whether the combination of in-service data acquisition methods and related crack growth analysis adequately account for ripple-type loads encountered in service.

REFERENCES

1. Pinckert, R. E., "Improved Fatigue Life Tracking Procedures for Navy Aircraft Structures - Phase I Final Report," Naval Air Development Center, Report No. NADC-77194-60, August, 1980.

2. Peterson, R. E., "Stress Concentration Factors," John Wiley and Sons, 1974.

3. Potter, J. M. and Noble, R. A., "A User's Manual for the Sequence Accountable Fatigue Analysis Computer Program," Air Force Flight Dynamics Laboratory Report No. AFFDL-TR-74-23, May, 1974.

4. Carroll, James R., et. al, "Investigation of Stress-Strain History Modeling at Stress Risers," Phase I, Air Force Flight Dynamics Laboratory Report No. AFFDL-TR-76-150, June, 1977.

5. Carroll, James R., et. al, "Investigation of Stress-Strain History Modeling at Stress Risers," Phase II, Air Force Flight Dynamics Laboratory Report No. AFFDL-TR-78-167, December, 1978.

6. Girolamo, R., Dumesnil, C. E., "New Fatigue Life Tracking Alternative for Navy Aircraft," Naval Air Development Center, Report No. NADC-79030-60, August, 1981.

7. Powell, B. E., Duggan, T. V., Jeal, R., "The Influence of Minor Cycles on Low Cycle Fatigue Crack Propagation," International Journal of Fatigue, Volume 4, No. 1, January, 1982.

NON-GOVERNMENT ACTIVITIES

	No. of Copies
ALCOA, ALCOA Labs, ALCOA Center, PA 15069 (Attn: Mr. J. G. Kaufman)	1
Battelle Columbus Labs, 505 King Avenue, Columbus, OH 43201 (Attn: Dr. B. Leis)	1
Boeing Commercial Airplane Co., P. O. Box 3707, Seattle, WA 98124 (Attn: Mr. T. Porter)	1
Douglas Aircraft Co., 3855 Lakewood Blvd., Long Beach, CA 90846 (Attn: Mr. Luce, Mail Code 7-21)	1
Drexel University, Phila., PA 19104 (Attn: Dr. Averbuch)	1
Fairchild Industries, Hagerstown, MD 21740 (Attn: Tech. Library)	1
General Dynamics, Convair Division, San Diego, CA 92138 (Attn: Mr. G. Kruse)	1
General Dynamics Corporation, P. O. Box 748, Ft. Worth, TX 76101 (Attn: Dr. S. Manning)	1
Grumman Aerospace Corporation, South Oyster Bay Road, Bethpage, L.I., NY 11714 (Attn: Dr. H. Armen)	
(Attn: Dr. B. Leftheris)	1
(Attn: Dr. H. Eidenoff)	1
Lehigh University, Bethlehem, PA 18015	
(Attn: Prof. G. C. Sih)	1
(Attn: Prof. R. P. Wei)	1
Lockheed-California Co., 2555 N. Hollywood Way, Burbank, CA 91520 (Attn: Mr. E. K. Walker)	1
Lockheed Georgia Co., Marietta, GA 30063 (Attn: Mr. T. Adams)	1
McDonnell Douglas Corporation, St. Louis, MO 63166	
(Attn: Mr. L. Impellizeri)	1
(Attn: Dr. R. Pinckert)	1
Northrop Corporation, One Northrop Ave., Hawthorne, CA 90250	
(Attn: Mr. Alan Liu)	1
(Attn: Dr. M. Ratwani)	1
Rockwell International, Columbus, OH 43216 (Attn: Mr. F. Kaufman)	1
Rockwell International, Los Angeles, CA 90009 (Attn: Mr. J. Chang)	1
Rockwell International Science Center, 1049 Camino Dos Rios, Thousand Oaks, CA 91360 (Attn: Dr. F. Morris)	1
Rohr Corporation, Riverside, CA 92503 (Attn: Dr. F. Riel)	1
Sikorsky Aircraft, Stratford, CT 06622	1
University of Dayton Research Institute, 300 College Park Ave., Dayton, OH 45469 (Attn: Dr. J. Gallagher)	1
University of Illinois, College of Engineering, Urbana, IL 61801 (Attn: Dept. of Mechanics and Industrial Eng., Profs. J. D. Morrow, D. F. Socie)	2
Vought Corporation, Dallas, TX 75265	
(Attn: Dr. C. Dumisnil)	1
(Attn: Mr. T. Gray)	1
University of Pennsylvania, Dept. of Mechanical Engineering and Applied Mechanics, 111 Towne Bldg. D3, Phila., PA 19104 (Attn: Dr. Burgers)	1

FAA

No. of
Copies

FAA, Washington, DC 20591 (Attn: J. R. Soderquist). . . .   1
FAA, Technology Center, Atlantic City, NJ 08405
  (Attn: Mr. D. Nesterok, ACT-330).   1

NASA

NASA, Langley Research Center, Hampton, VA 23365
  (Attn: Mr. H. Hardrath)   1
NASA, Washington, DC 20546 (Attn: Airframes Branch, FS-120)   1
NASA, Lewis Research Center, Cleveland, OH 44135
  (Attn: Technical Library)   1
NASA, George C. Marshall Space Flight Center, Huntsville,
  AL 35812 (Attn: Technical Library).   1

USAF

AFWAL, WPAFB, OH 45433
  (Attn: AFWAL/FIBE).   1
  (Attn: FIBEC)   1
  (Attn: FIBAA)   1
  (Attn: AFWAL/FIB)   1
Ogden ALC, Hill AFB, UT 84055 (Attn: MANCC)   1
Oklahoma City ALC, Tinker AFB, OK 73145 (Attn: MAQCP) . .   1
Sacramento ALC, McClellan AFB, CA 95652 (Attn: MANE) . .   1
San Antonio ALC, Kelly AFB, TX 78241 (Attn: MMETM). . . .   1
Warner Robbins ALC, Robins AFB, GA 30198
  (Attn: MMSRD/Dr. T. Christian).   1

U. S. Army

Applied Technology Laboratory, USARTL (AVRADCOM), Fort
  Eustis, VA 23604 (Attn: H. Reddick)   1
U. S. Army Materials and Mechanics Research Center
  (DRXMR-PL), Watertown, MA 02172.   1
U. S. Army Research Office, Durham, NC 27701   1

INFO. SERVICES

DTIC, Cameron Station, Alexandria, VA 22314   12
MCIC, Battelle Columbus Laboratories, 505 King Avenue,
  Columbus, OH 43201   1
NTIS, U. S. Dept. of Commerce, Springfield, VA 22151 . . .   2

DATE

ILME